

## Research Article

# FE Simulation of Transmission Tower

**Boshra Eltaly, Amen Saka, and Kamel Kandil**

*Civil Engineering Department, Faculty of Engineering, Minufiya University, P.O. Box 32511, Shebin Al-Kom, Minufiya, Egypt*

Correspondence should be addressed to Boshra Eltaly; [boshra\\_eltaly@yahoo.com](mailto:boshra_eltaly@yahoo.com)

Received 6 January 2014; Accepted 10 February 2014; Published 10 June 2014

Academic Editor: John Mander

Copyright © 2014 Boshra Eltaly et al. This is an open access article distributed under the Creative Commons Attribution License, which permits unrestricted use, distribution, and reproduction in any medium, provided the original work is properly cited.

The vital components of the transmission line are the electrical transmission towers. They are commonly used to support the phase conductors and shield wires of a transmission line. Also the accurate prediction of tower failure is very important for the reliability and safety of the transmission system. The current research describes nonlinear FE models of predicting the transmission tower failure. In the current FE simulations, the eccentricity and the joint effect of the tower were considered. The current models have been calibrated with results from previous full-scale tower tests and numerical models with good accuracy in terms of both the failure load and the failure mode.

## 1. Introduction

The common transmission towers systems are the pole system and the lattice system. The pole system can be economically used for relatively shorter span and lower voltage (345-kV or less). It may be wood pole, tubular steel, concrete, or reinforced plastics pole (it is the highest restricting application). On the other hand the lattice system can be used for the highest voltage level. The lattice tower members typically consist of steel or aluminum angle sections. The two types can be self-supporting or guyed [1, 2]. In 2012, Selvaraj et al. [3] discussed experimental studies carried out on transmission line tower made from FRP pultruded sections.

The tower must be designed for their own weight, weight of the conductors and insulators, wind, ice (eighty-two transmission towers in the end of November 2005 in Münsterland, Germany failed due to snow rolls formed around the conductors [4]), vibration load, and security load. The security load occurs on the tower due to accidental events such as broken conductors, broken insulators, or collapse of an adjacent structure in the line due to an environmental event such as a tornado. It causes longitudinal loads on the tower [5].

The primary members of the lattice tower are the leg and the bracing members. They carry the vertical and shear loads on the tower and transfer them to its foundation. Secondary or redundant bracing members are used to provide

intermediate support to the primary members to reduce their unbraced length and increase their load carrying capacity [2]. The tower members are usually angles or flat bars and they are often directly connected together to eliminate gussets by galvanized bolted joints. Using galvanized bolted joints reduces effectiveness of friction type so that these bolts are bearing type bolts. Additionally bearing type bolts are preferred to friction type because they are easy to erect at heights, they are economical; the tower members are thin, and fatigue effects are controlled by limiting slenderness ratio of members and use of lock washers to prevent nut loosening [6].

Most of the latticed towers presently in service around the world were analyzed as a space truss. Each member of the lattice tower is assumed to be pin-connection at its joints carrying only the axial load and no moment (linear ideal truss analysis). Then the tower is designed to carry axial compression and tensile forces. The full-scale transmission tower tests give larger deflection than the theoretical linear elastic analysis. Also it was found that almost 25% of the towers tested failed below the design loads and often at unexpected locations. Additionally their results showed that the local buckling occurred as a result of the bending moment caused by unbalanced deformation as well as axial compression [7–10].

Several researches developed numerical and theoretical models to represent the transmission tower. Prasad Rao

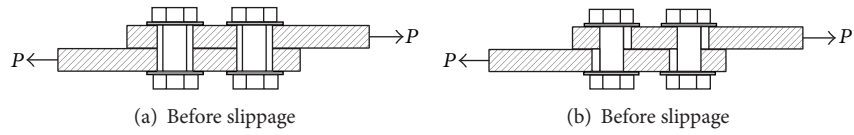


FIGURE 1: Bolted joint slippage effects.

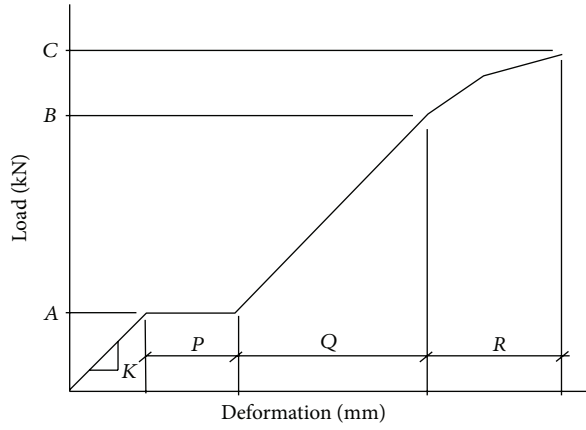


FIGURE 2: Ungkurapinan et al. single-leg bolted joint [18].

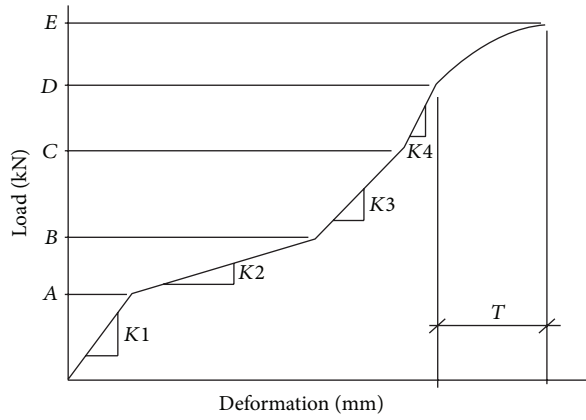


FIGURE 3: Ungkurapinan et al. lap-splice bolted joint model [18].

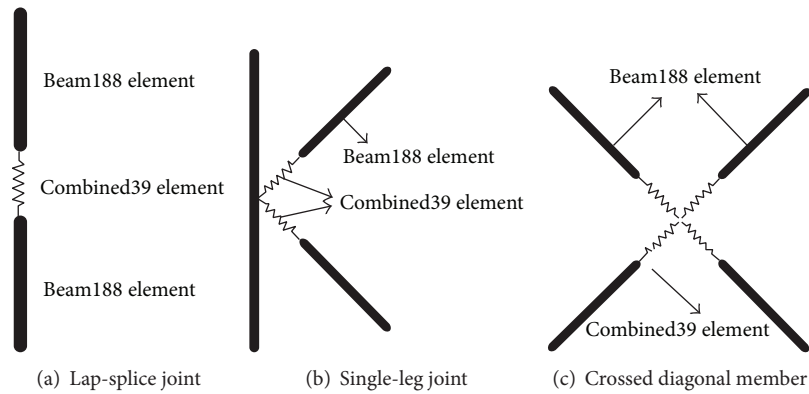


FIGURE 4: Joint slippage model.

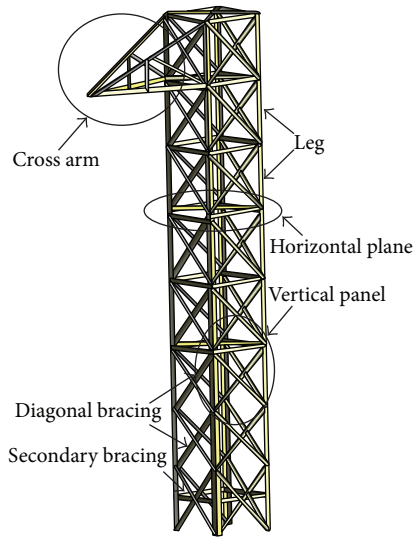


FIGURE 5: Three dimensional view of studied tower 1.

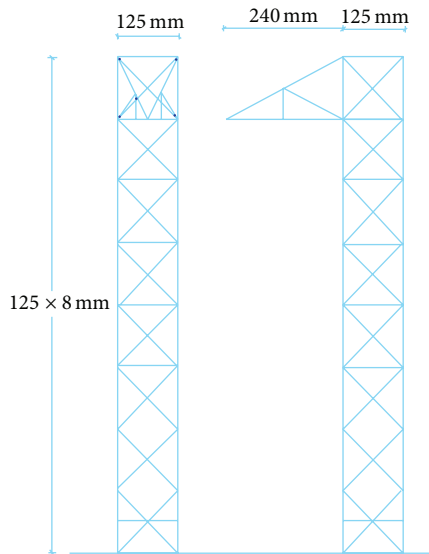


FIGURE 6: Dimension of studied tower 1.

and Kalyanaraman [11] developed nonlinear numerical analysis using finite element method. They represented only the main leg members of the tower. Two types of joint models were investigated. In the two models, the angle of the members was modeled using flat-shell elements. In the first model, the joints were assumed to be rigid by using rigid elements between the bolt lines (it was represented by beam element) and the centroid of the angle members. The second model is a flexible joint model. In it, the contact force transfer between the legs of the angles was modeled using the gap elements. The bolts in the joint were modeled using a rod element. Albermani and Kitipornchai [12] developed a new analytical technique. This model represents geometric and material nonlinearities for simulating ultimate structure of the lattice transmission tower. In their model all the members of the tower were represented by beam-column element.

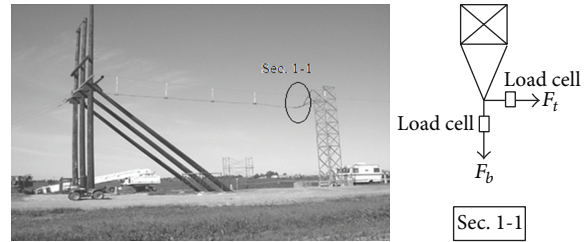


FIGURE 7: Experimental test site of Lee and McClure [19] tower.

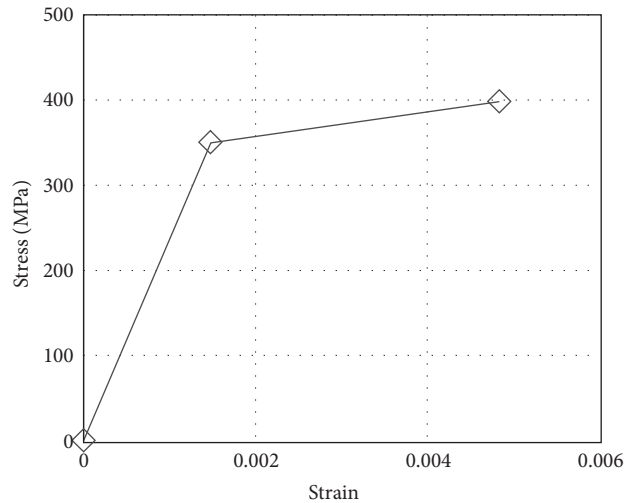


FIGURE 8: Stress-strain curve of tower 1 material.

In the analysis process, an incremental-iterative predictor-corrector solution strategy is used. Comparing the results of their new technique and the results of their experimental model showed that the technique has been shown to predict accurately both the failure load and the failure mode.

More studies such as Kitipornchai et al. [13], Knight and Santhakumar [14], Ahmed et al. [15], and Albermani et al. [16] indicated that the bolted joint effects (joint slippage) has a significant influence on tower behavior by either reducing its load-carrying capacity or increasing deflections under working loads and this effect is not considered in the linear ideal truss analysis. Joint slippage is the relative displacement of very low stiffness and bearing type bolted (see Figure 1). Also it occurs since bolt holes are drilled in an oversize manner to provide an erection tolerance of 1.6 mm (1/16 in).

The current paper presented theoretical study depending on the finite element method (FEM) using ANSYS software package [17] to predict the actual strength and failure mechanism of the transmission tower. In the current models, L-section beam finite elements considering the combinations of biaxial bending, axial stretch, and shearing behaviors were used to present the tower members. Also the current model considered geometry and material nonlinearities. Additionally eccentricities of connections for the tower members that they connected only on one leg and joint slippage were modeled.

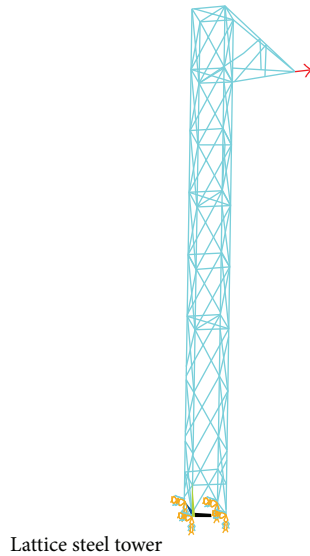


FIGURE 9: FE simulation of studied tower 1.

## 2. Finite Element Simulation

In the current work, two theoretical models were developed using ANSYS version 12 package. In the current developed simulation models, the tower members were represented by their real cross section (L-section) using Beam188 elements. Beam188 element has six degrees of freedom at each node; translations and rotations in the nodal  $x$ ,  $y$ , and  $z$  directions [17]. This element is well-suited for large rotation or large strain nonlinear applications. Also both of the geometry and material nonlinearity was considered in this model. The material nonlinearity is represented by multilinear kinematic hardening constants (MKIN). It assumes the total stress range is equal to twice the yield stresses, so that Bauschinger effect is included. MKIN may be used for materials that obey von Mises yield criteria. Von Mises yield criteria include most metals. The material behavior is described by a stress-strain curve starting at the original and it has positive stress and strain values. The initial slope of the curve is represented by the elastic modulus of the material.

In ANSYS [17] nonlinear analysis, two different techniques may be used. The first technique is load-control technique. In this technique, total load is applied to a finite element model. The load is divided into a series of load increments during the analysis called load steps. The second technique is displacement-control technique. In this technique, the displacement is applied to the model and the displacement is divided into a series of increments called load steps. The load steps are defined by program user. With increasing the number of load steps, the accuracy of results is increased and the program needs a long time to complete the solution. After completing each increment, the stiffness matrix of the model is adjusted to reflect nonlinear changes in structural stiffness. This changes occurs before proceeding to the next load increment. In the current analysis, load-control technique is used.

The ANSYS [17] uses Newton-Raphson method for updating the model stiffness. Before each solution, the Newton-Raphson method evaluates the out-of-balance load vector. The out-of-balance load vector is the difference between the restoring forces (the load corresponding to the element stresses) and the applied loads. The program then performs a linear solution, using the out-of-balance loads and checks for convergence. If convergence criteria are not satisfied, the out-of-balance load vector is reevaluated, the stiffness matrix is updated, and a new solution is obtained. This iterative procedure continues until the solution converges. A number of convergence enhancement and recovery features, such as line search and automatic load stepping can be activated to help the problem to converge. If convergence cannot be achieved, then the program attempts to solve with a smaller load increment.

In the current model 1, the influence of the joint effect was not considered and it was considered in model 2. The joint effect is represented in model 2 by Combin39 element. It is a unidirectional element with nonlinear generalized force-deflection capability that can be used in any analysis. The element has longitudinal or torsional capability in 1-D, 2-D, or 3-D applications. The longitudinal option is a uniaxial tension-compression element with up to three degrees of freedom at each node, translations in the nodal  $x$ ,  $y$ , and  $z$  directions. The torsional option is a purely rotational element with three degrees of freedom at each node: rotations around the nodal  $x$ ,  $y$ , and  $z$ -axes.

In the current model 2, joint slippage was modeled as Ungkurapinan et al. [18]. They pointed that the joint slippage is influenced by the applied load and diameter, pitch, numbers (1–4 bolts), arrangement, length, and properties of bolt. Also it is influenced by poor workmanship. They presented an experimental test for bearing bolted joint that was used in the lattice towers (two members were joined directly). In their experimental program, the load applied was measured and poor workmanship was varied to include three settings namely: maximum construction clearance (3.2 mm), normal construction clearance (1.6 mm), and joints set in bearing (0 mm clearance). End distance and edge distance between bolts were 25.4 mm and 51 mm, respectively. Pitch of bolts was held in a constant manner at 51 mm. Bolt diameter was 16 mm. Their specimens were placed centrally in the testing machine (Hydraulic Testing Machine) and this caused the generation of a couple which turned the entire bolted joint relative to outer member ends due to the eccentricity of loading. From their results, they illustrated the joint effects by idealized curve of load versus joint deformation as shown in Figures 2 and 3 and Tables 1 and 2.

In current model 2, each member of the tower legs is represented by Beam188 elements. The bracing members were represented by Beam188 elements along their length and at each end node of the member; six nonlinear springs (Combin39 elements) are defined (see Figure 4). The nonlinear spring has translational stiffness along  $x$ ,  $y$ ,  $z$ , and rotational stiffness around  $x$ ,  $y$ , and  $z$ . As listed in Table 3, joint slippage effects are considered by prescribing the axial stiffness  $K_x$  which varies depending on the joint type as presented in Table 1 and Figure 2. Also at lap-splice of the leg, six nonlinear

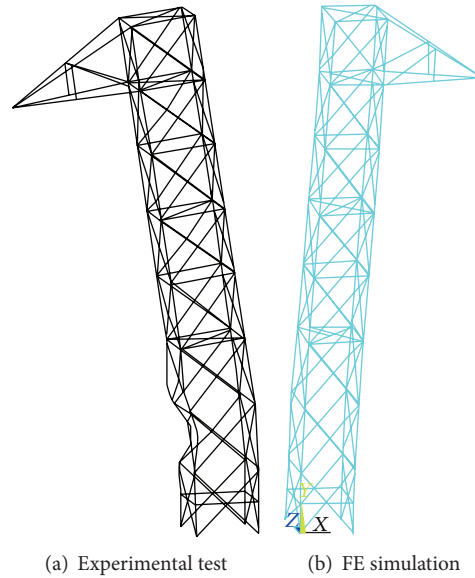


FIGURE 10: Deformed shapes from the bending test.

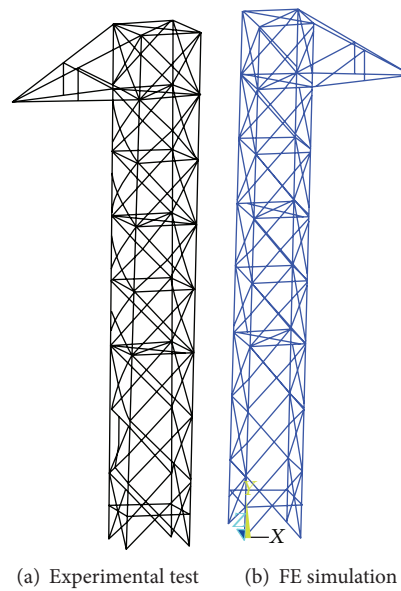


FIGURE 11: Deformed shapes from the torsional test.

springs are defined as in Table 3 and the stiffness of the axial spring is illustrated in Table 2 and Figure 3.

### 3. Towers Studied

Two different towers were studied in the current research to evaluate the new FE models.

**3.1. Tower 1.** This tower was experimentally and theoretically studied by Lee and McClure [19]. The overall view of the tested prototype is depicted in Figure 5. The height of the tower is 10000 mm. The tower consists of 8 panels with

a square base of 125 mm  $\times$  125 mm in each face of the tower as illustrated in Figure 6. All members are hot-rolled single angle shapes. The largest leg size is 89 mm  $\times$  89 mm  $\times$  6.4 mm. Table 4 shows the section sizes of the angle members used.

The load was applied at the cross-arm tip of the tower by pulling it using a towing truck in two directions ( $x$  &  $y$ ). The tower is subjected to the transverse load  $F_b$ , in the direction parallel to the axis of symmetry ( $-y$  direction), to create an overall bending effect. Also the loading  $F_t$  is applied to be perpendicular to the cross arm ( $x$  direction) to investigate the flexural-torsional behavior of the structure (see Figure 7). The load magnitude was measured by a load-cell as shown schematically in Figure 6. Lee and McClure [19] measured

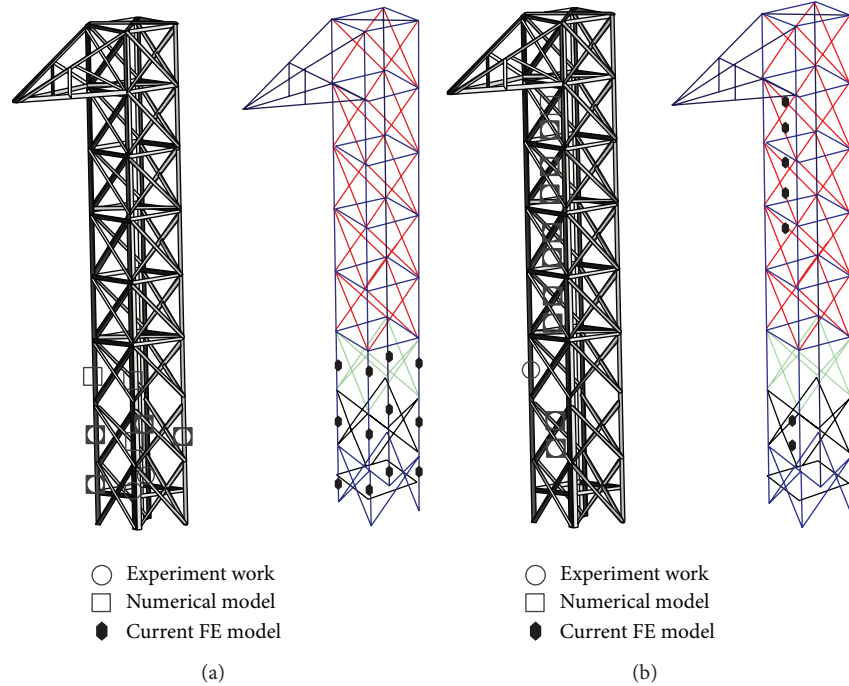


FIGURE 12: Members failing in Lee and McClure [19] experimental results and numerical solution and the current FE simulations (a) bending case, (b) flexure-torsion case.

TABLE I: Ungkurapinan et al. single-leg bolted joint [18].

Numer of bolts per joint	A (kN)	Slope (kN/mm)	P (mm)			Q (mm)	B (kN)	R (kN)	C (kN)
			Maximum clearance	Normal clearance	Bearing				
1	9.29	27.51	2.21	0.85	0	2.74	65.03	6.04	107.8
2	20.14	84.81	2.21	0.85	0	1.73	91.51	2.55	157.7
3	29.28	113.9	2.21	0.85	0	2.4	152.9	2.18	204.4
4	46.95	139.0	2.21	0.85	0	1.85	168.2	1.16	207.6

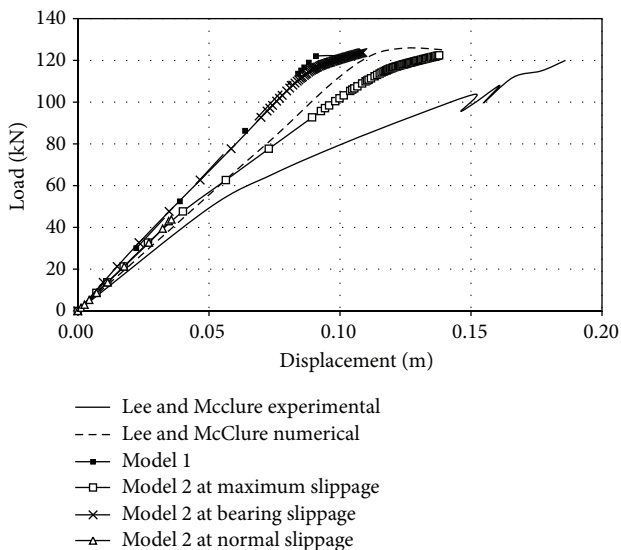


FIGURE 13: Load-displacement curves in the bending case.

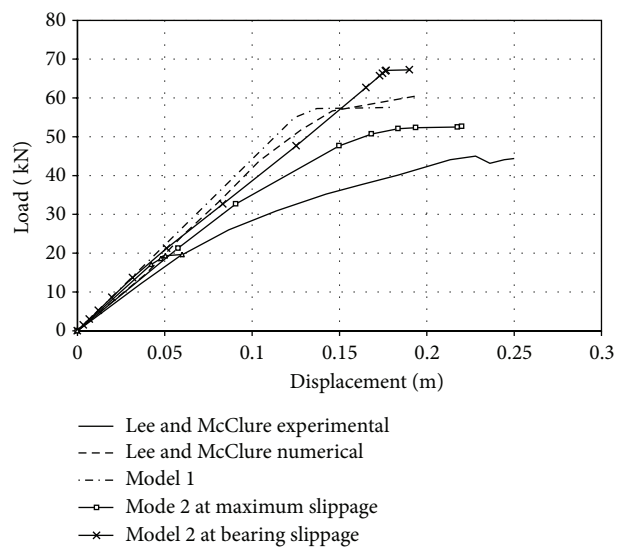


FIGURE 14: Load-displacement curves in the flexural-torsion case.

TABLE 2: Ungkurapinan et al. lap-splice bolted joint model [18].

Clearance	Load (kN)						Slope (kN/mm)			T (mm)
	A	B	C	D	E	K1	K2	K3	K4	
Maximum	43.28	117.77	216.4	285.15	299.68	263.45	20.99	43.65	86.55	0.36
Normal	43.28	79.49	216.4	285.15	299.68	263.45	20.99	43.65	86.55	0.36
Bearing	43.28	0	216.4	285.15	299.68	263.45	0	43.65	86.55	0.36

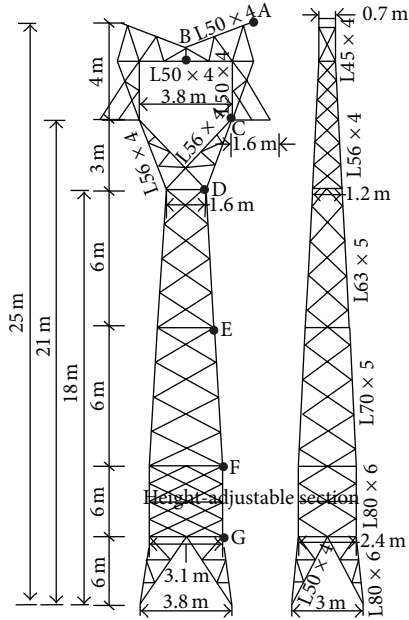


FIGURE 15: Tower studied 2 geometry outlines.

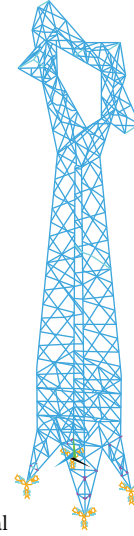


FIGURE 17: FE simulation of tower 2.

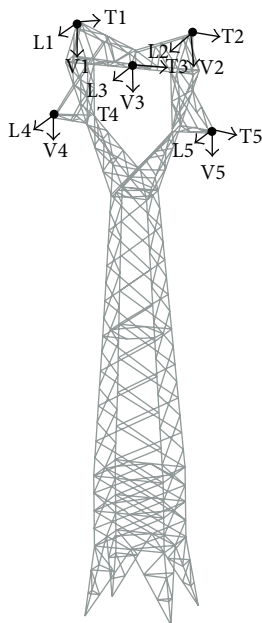


FIGURE 16: Loading points of studied tower 2.

TABLE 3: Joint stiffness models.

Stiffness	Single bolt	Two and more bolts
$K_x$	Semirigid	Semirigid
$K_y$	Rigid	Rigid
$K_z$	Rigid	Rigid
$K_{rot x}$	Rigid	Rigid
$K_{rot y}$	Pin	Rigid
$K_{rot z}$	Rigid	Rigid

TABLE 4: Cross section dimensions of studied tower number 1 (unite is mm).

Legs	Diagonal bracings	Horizontal panels
89 × 89 × 6.4	64 × 51 × 4.8	64 × 51 × 4.8
76 × 76 × 6.4	51 × 51 × 3.2	51 × 51 × 4.8
	51 × 48 × 3.2	
	44 × 44 × 3.2	

the cross-arm tip displacement from images taken by a high-speed camera installed right beneath the cross-arm tip on the ground. Also, sixteen video cameras were installed on each face of the tower so that images of each vertical panel along the four sides would be recorded to identify the failure sequence with the help of the strain gage readings.

Lee and McClure [19] developed three numerical models for simulating behavior of the tested tower. In their models,

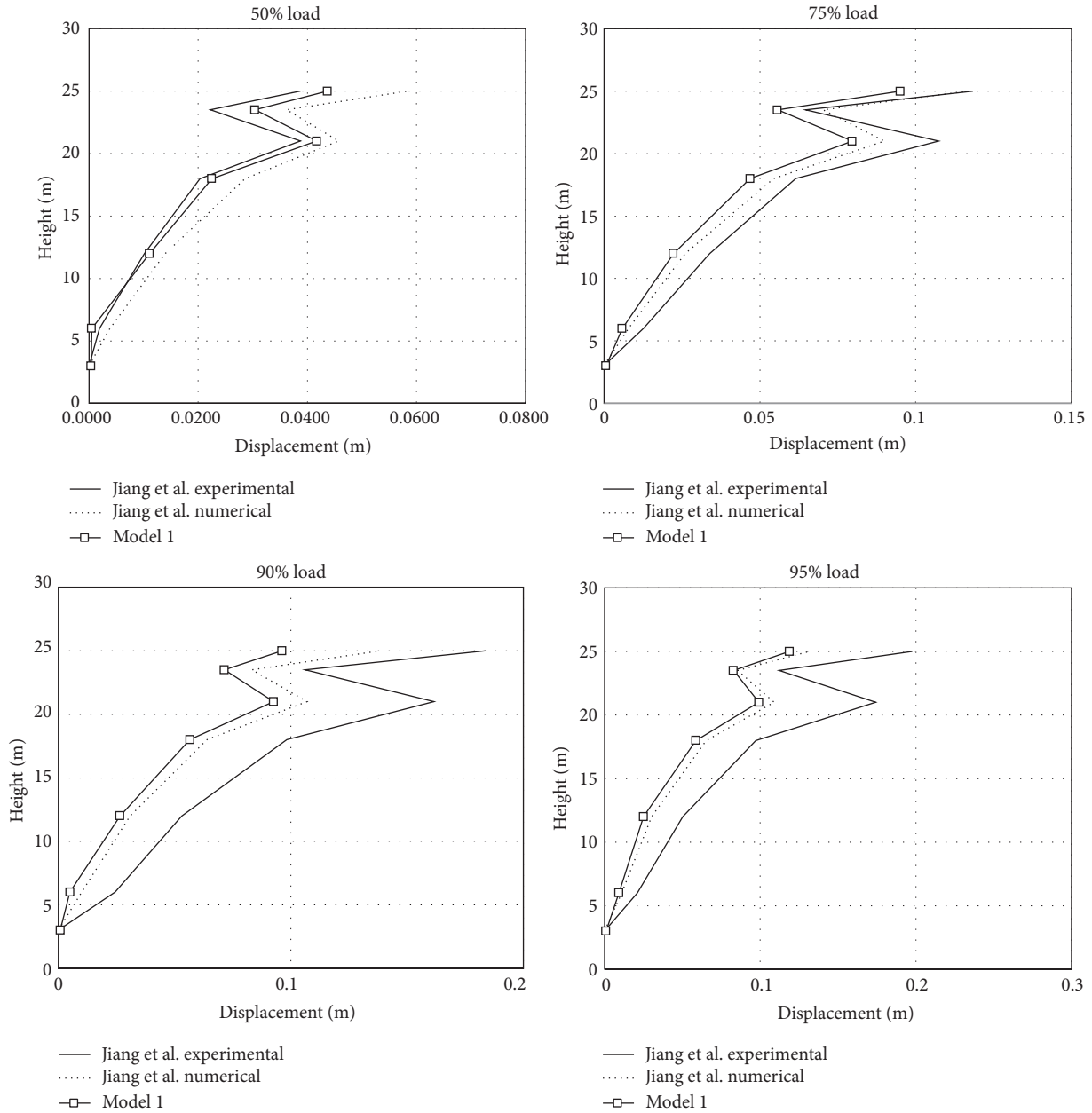


FIGURE 18: Tower 2 longitudinal displacement at no joint slippage (model 1).

the tower members were represented by the 2-node three-dimensional L-section beam finite elements available in the ADINA user subroutine. In their first model, they used pin-joint for one-bolt connections and rigid-joint for connections using two or more bolts and they modeled the eccentricities at beam ends. The second model is the same as the first model but the eccentricity is not considered. In the third model, the eccentricity is modeled as in Model-I but all connections are considered rigid. Their numerical model considering both geometry and material nonlinearities (using the Pushover analysis) and the full Newton-Raphson method was used. In the current research, their first model is used in comparing the results of the current FE simulations because this model gives the nearest results to experimental results.

Figures 8 and 9 present the stress-strain curve of the tower material and the current FE simulation, respectively. The tower models are assumed to be fixed on a rigid base.

In the current sections, the results of tower 1 are presented and discussed. Figures 10 and 11 illustrate deformed shape of the studied tower 1 in bending and flexure-torsional case, respectively as obtained from Lee and McClure [19] experimental and numerical work and the two current FE models. Figure 12 presents the members failing from the experimental test and the theoretical models. From Figure 12, it can be observed that in the bending case, failures are concentrated at the base of the main legs, while the diagonal members of the tower below the cross arm fail in the flexure-torsion case. From Figure 12, it can be observed that

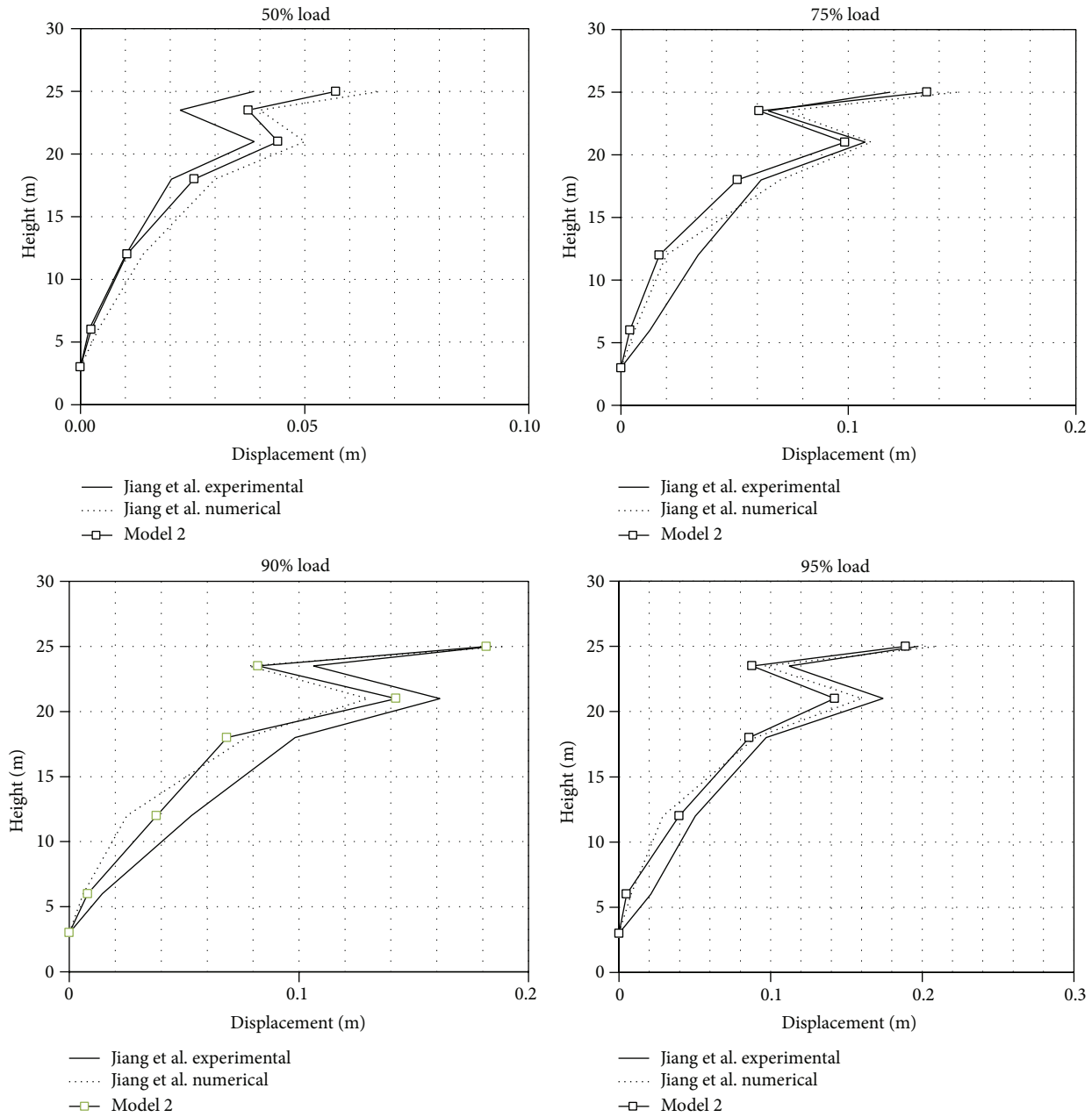


FIGURE 19: Tower 2 longitudinal displacement at maximum construction.

the symmetric failure mode is obtained in Lee and McClure [19] numerical model and the current FE simulation. On the other hand the experimental result shows nonsymmetric failure behavior.

Figure 13 displays the load-displacement curve at tip point of tower 1 studied from Lee and McClure experimental and numerical [19] work and the current FE simulations in the bending case. Also Figure 14 presents the relationship between the load and displacement at the same point in the case of flexural-torsion from Lee and McClure experimental and numerical [19] work and current FE simulations. These figures show increasing gaps between the Lee and McClure [19] experimental results, their numerical results, and current

model 1 and model 2 in the cases of bearing and normal joint slippage. Additionally from these figures, it can be clearly seen that considering joint slippage with maximum clearance (model 2 at maximum slippage) decreases the gap between the experimental and the current FE simulation results.

The difference between the experimental results and the current FE simulations can be referred to the movement of the foundation as observed by Lee and McClure [19] in the full-scale test and the foundation was considered as rigid joint in the FE simulations. Furthermore Lee and McClure [19] mentioned that there were many possible unknown imperfections in the real tower structures tested and their numerical studies and the current FE simulations did not

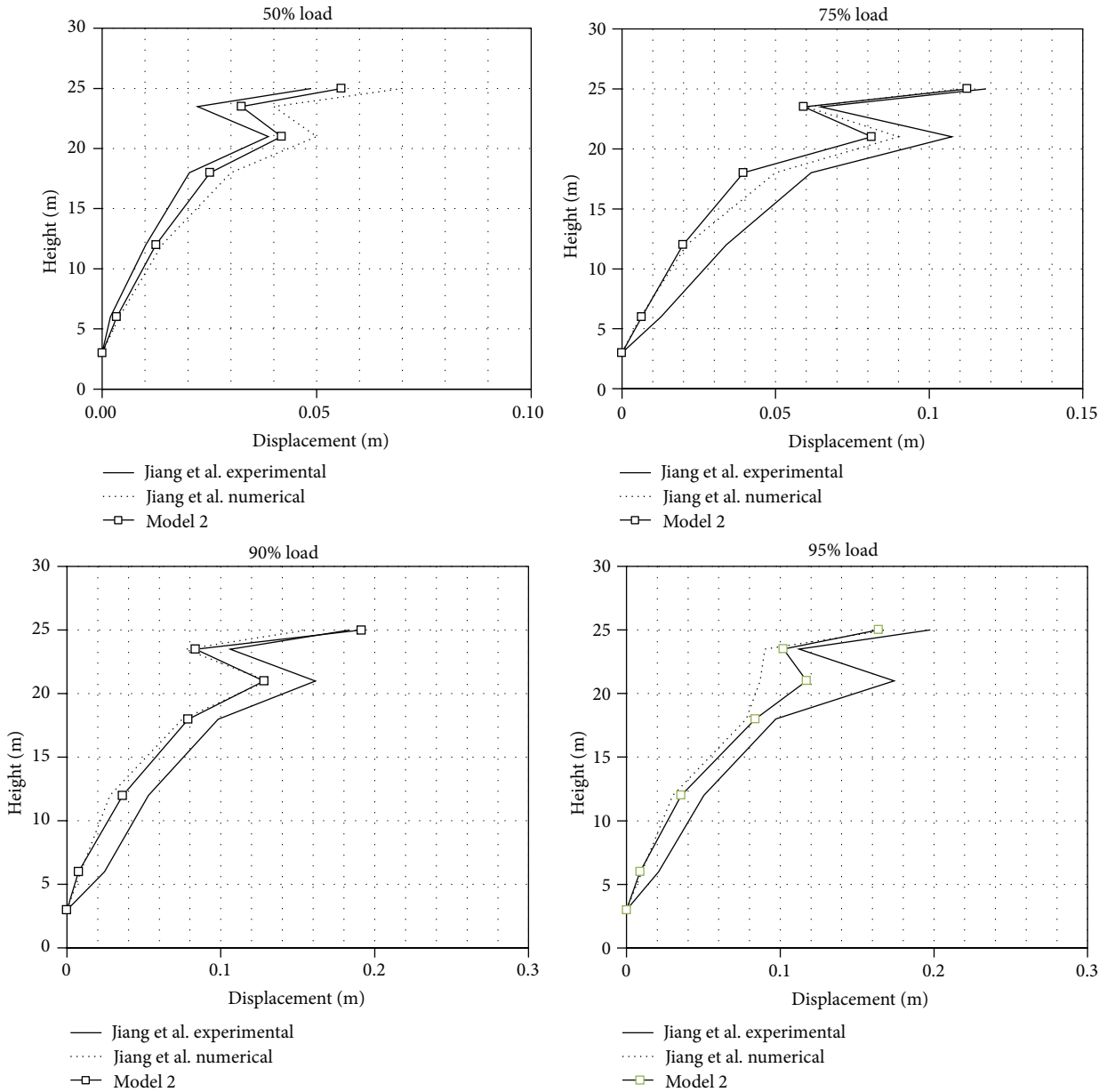


FIGURE 20: Tower 2 longitudinal displacement at normal construction clearance.

consider any artificial imperfection in the numerical model. These unknown imperfections induce the nonsymmetric behavior of the real structures in the bending case. Also some dynamic effects were involved in the experimental results as noted by Lee and McClure [19]. However, their numerical solutions and the current models were obtained by static analysis.

3.2. *Tower 2.* In 2007 and 2009 at the China Electric Power Research Institute in Beijing, static prototype tests were conducted on a 25 m tall 110 kV height-adjustable transmission tower used in subsidence-prone area due to coal mining. Their experimental results were published in 2011 by Jiang et al. [20]. The outline of the tower geometry and the loading

points are shown in Figures 15 and 16, respectively. The loading directions in Figure 16 refer to longitudinal (L), transverse (T), and vertical (V). The loading case applied during the tests is listed in Table 5. Figure 15 identifies points A, B, C, D, E, F, and G at which the corresponding deflections were recorded experimentally. The steel material properties specified in the current numerical model are the nominal values used in design: a Young's modulus of 200 GPa and a yield stress of 235 MPa for all members.

Jiang et al. [20] developed numerical models that include joint eccentricity effects and different joint slippage models by USFOS program. They represented the individual members by beam element with angle shapes. In their models, the material nonlinearity was considered and it was based on

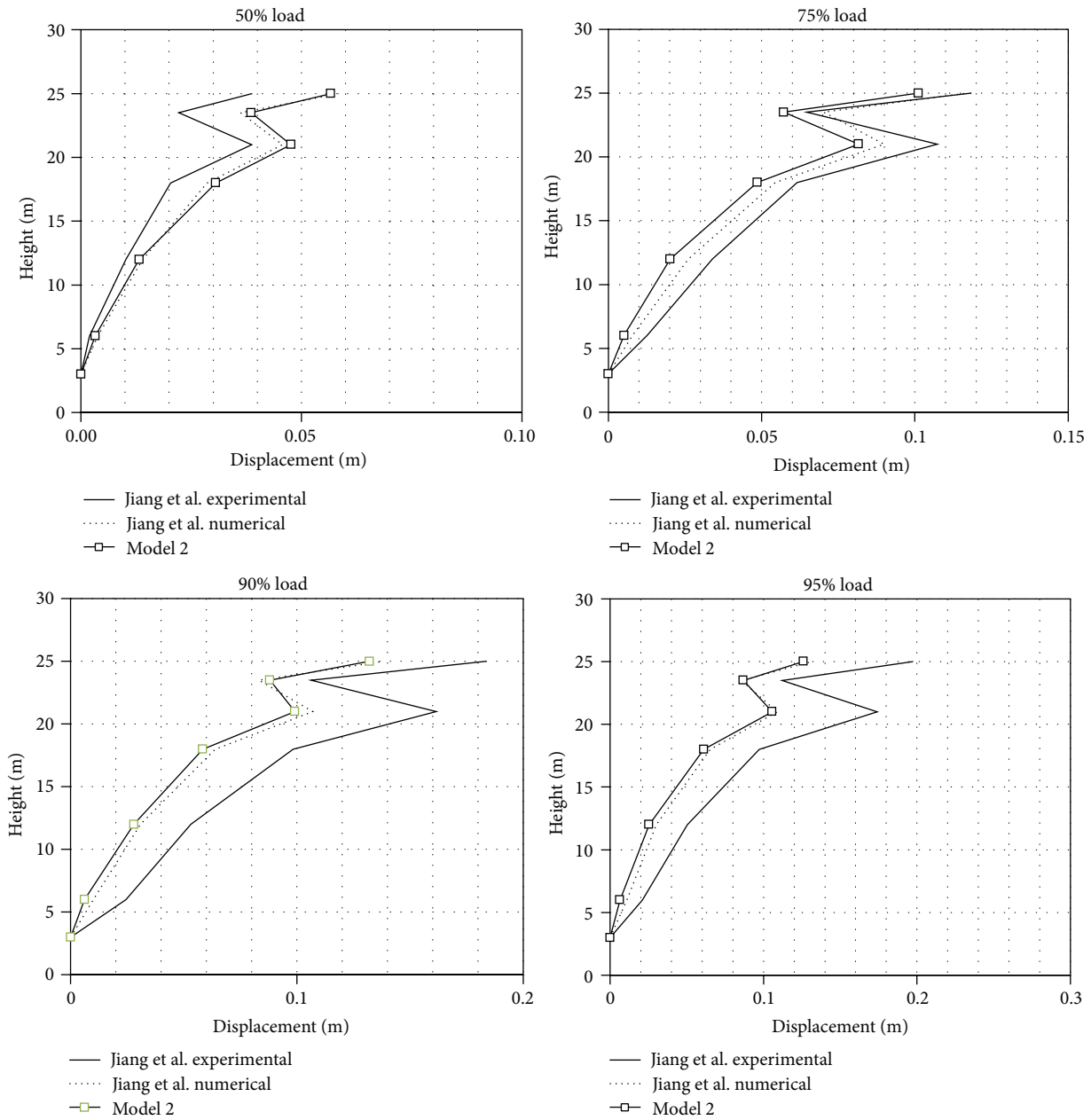


FIGURE 21: Tower 2 longitudinal displacement at bearing construction clearance.

the plastic hinge theory. In this theory, plastic hinges may be introduced at both ends and midspan of each member. When the analysis indicates the onset of yielding in a member, a plastic hinge is inserted at the corresponding element node. If yielding is taking place at midspan of the element, the member is automatically split into two new subelements connected by a plastic hinge and the stiffness matrix for the two subelements is assembled. In their models, the joint effects were represented by six springs at the end of the joint with rigid translational stiffness along  $y, z$ , rigid rotational stiffness around  $x, y, z$  and axial stiffness along  $x$  depending on the type of joint slippage as Ungkurapinan et al. [18]. Jiang et al. [20] used maximum experimental load and reached 95%

of the design load as the reference value in comparison with numerical predictions. The tower did not collapse during the test, so the maximum experimental load is not the collapse load. This load is used in the current FE simulations. The current FE simulation is presented in Figure 17.

In the below sections, comparing results of the current FE simulations with Jiang et al. [20] experimental and numerical results are presented and discussed. The longitudinal tower displacements at different height of the tower and at different percentage of applied load (50%, 75%, 90%, and 95% load) are reported in Figure 18 to Figure 22. Figure 18 represents the lateral displacement as obtained from the Jiang et al. [20] test, their numerical model without considering the joint effect,

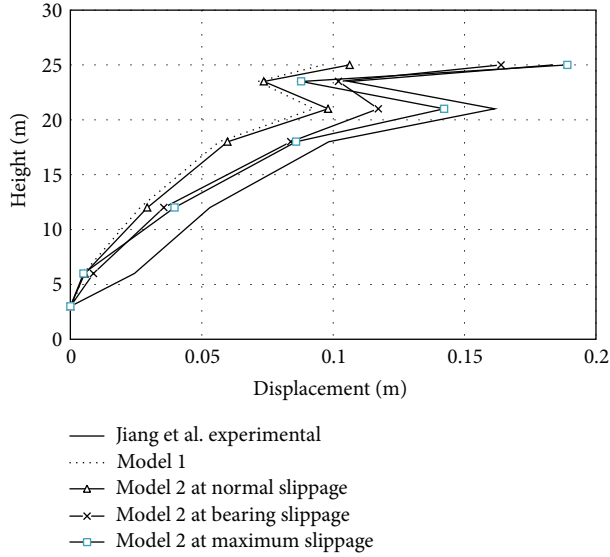


FIGURE 22: Tower 2 longitudinal displacement at 95% load.

TABLE 5: Experimental conductor breakage loading for tower studied.

	Point				
	1	2	3	4	5
Load (kN)					
Direction					
Transverse	0.00	0.00	0.00	0.00	0.00
Longitudinal	0.00	0.00	0.00	0.00	15.75
Vertical	1.82	1.82	5.00	5.00	5.00

and the current model 1. From this figure, it can be concluded that the current model 1 gives similar lateral displacement to Jiang et al. [20] numerical lateral displacement. Also this figure shows that when the load is relatively small (at 50% load) the lateral displacement from the current model 1 agrees with the experimental results. The given lateral displacement at point A from the test is 0.95 time current model 1 displacement. However, as the load is increased (at 90% and 95%) this agreement is progressively lost. The current model 1 gives lateral displacement at point A less than the lateral displacement at this point from the experimental program by 40%.

Additionally Figure 19 to Figure 20 that represent the comparison between lateral displacement from the experimental test and both of Jiang et al. [20] numerical and model 2 with different joint clearance: maximum, normal and bearing, respectively, showed the agreement of results of the current FE simulation considering the joint effect with Jiang et al. [20] numerical models results. These figures also illustrated that the tower deformations given from the FE model that considered joint slippage with maximum construction clearance are closer to measured displacements during the test and this conclusion also appeared in Figure 21.

## 4. Conclusion

Two FE models were developed in the current research to study the nonlinear behavior of electrical transmission towers under static load. The tower was modeled by the 2-node three-dimensional L-section beam finite elements and both of the geometrical and material nonlinearities were considered in the current FE simulations. Model 1 did not consider the eccentricity of connections for the tower members and the joint slippage. In model 2, both of the eccentricity of connections for the tower members and the joint slippage were modeled. The FE simulations results were compared with the previous published results of the full-scale experimental tests and the numerical solutions that were carried out on two different towers. The conclusions from the current study can be summarized as follows.

- (1) The current model 2 in the case of maximum joint slippage shows excellent agreement with the experimental test results of the two towers studied. The difference between the current FE simulations and tower 1 test results is due to not considering in the model the movement of the foundation during the test, unknown imperfections in the tower structure, and the dynamic effects in the experimental results.
- (2) In general, the behavior of connections of the tower structures has a direct effect on the ultimate behavior of the lattice steel tower structures but has not affected its failure modes and sequence.
- (3) Model 2 is very attractive to predict the ultimate behavior of the lattice steel tower structures.

## Conflict of Interests

The authors declare that there is no conflict of interests regarding the publication of this paper.

## References

- [1] D. G. Fink and H. Wayne Beaty, *Standard Handbook for Electrical Engineers*, Chapter 14: Overhead Power Transmission, McGraw-Hill, New York, NY, USA, 11th edition, 1978.
- [2] S. J. Fang, S. Roy, and J. Kramer, "Transmission structures," in *Structural Engineering Handbook*, W.-F. Chen, Ed., CRC Press LLC, Boca Raton, Fla, USA, 1999.
- [3] M. Selvaraj, S. Kulkarni, and R. Ramesh Babu, "Behavioral analysis of built up transmission line tower from FRP pultruded sections," *International Journal of Emerging Technology and Advanced Engineering*, vol. 2, no. 9, pp. 39–47, 2012.
- [4] C. Klinger, M. Mehdiانpour, D. Klingbeil, D. Bettge, R. Häcker, and W. Baer, "Failure analysis on collapsed towers of overhead electrical lines in the region Münsterland (Germany) 2005," *Engineering Failure Analysis*, vol. 18, no. 7, pp. 1873–1883, 2011.
- [5] A. C. I. Committee 318, *Building Code Requirements for Reinforced Concrete with Commentary*, American Concrete Institute (ACI), Detroit, Mich, USA, 1995.
- [6] A. Ungkurapinan, *Study of joint slip in galvanized bolted angle connections [M.S. thesis]*, University of Manitoba, Manitoba, Canada, 2000.

- [7] S. Roy, S.-J. Fang, and E. C. Rossow, "Secondary stresses on transmission tower structures," *Journal of Energy Engineering*, vol. 110, no. 2, pp. 157–172, 1984.
- [8] W. Peterson, "Design of EHV steel tower transmission lines," *Journal of Structure Division: Procedure of American Society Civil Engineering*, vol. 88, pp. 39–65, 1962.
- [9] M. Marjerrison, "Electric transmission tower design," *Journal of Structure Division: Procedure of American Society Civil Engineering*, vol. 94, pp. 1–23, 1968.
- [10] B.-W. Moon, J.-H. Park, S.-K. Lee, J. Kim, T. Kim, and K.-W. Min, "Performance evaluation of a transmission tower by substructure test," *Journal of Constructional Steel Research*, vol. 65, no. 1, pp. 1–11, 2009.
- [11] N. Prasad Rao and V. Kalyanaraman, "Non-linear behaviour of lattice panel of angle towers," *Journal of Constructional Steel Research*, vol. 57, no. 12, pp. 1337–1357, 2001.
- [12] F. G. A. Albermani and S. Kitipornchai, "Numerical simulation of structural behaviour of transmission towers," *Thin-Walled Structures*, vol. 41, no. 2-3, pp. 167–177, 2003.
- [13] S. Kitipornchai, F. G. A. Al-Bermani, and A. H. Peyrot, "Effect of bolt slippage on ultimate behavior of lattice structures," *Journal of Structural Engineering*, vol. 120, no. 8, pp. 2281–2287, 1994.
- [14] G. M. S. Knight and A. R. Santhakumar, "Joint effects on behavior of transmission towers," *Journal of Structural Engineering*, vol. 119, no. 3, pp. 698–712, 1993.
- [15] K. I. E. Ahmed, R. K. N. D. Rajapakse, and M. S. Gadala, "Influence of bolted-joint slippage on the response of transmission towers subjected to frost-heave," *Advances in Structural Engineering*, vol. 12, no. 1, pp. 1–17, 2009.
- [16] F. Albermani, S. Kitipornchai, and R. W. K. Chan, "Failure analysis of transmission towers," *Engineering Failure Analysis*, vol. 16, no. 6, pp. 1922–1928, 2009.
- [17] ANSYS, *Help and Manual*, ANSYS, Philadelphia, Pa, USA, 11th edition, 2006.
- [18] N. Ungkurapinan, S. R. D. S. Chandrakeerthy, R. K. N. D. Rajapakse, and S. B. Yue, "Joint slip in steel electric transmission towers," *Engineering Structures*, vol. 25, no. 6, pp. 779–788, 2003.
- [19] P.-S. Lee and G. McClure, "Elastoplastic large deformation analysis of a lattice steel tower structure and comparison with full-scale tests," *Journal of Constructional Steel Research*, vol. 63, no. 5, pp. 709–717, 2007.
- [20] W. Q. Jiang, Z. Q. Wang, G. McClure, G. L. Wang, and J. D. Geng, "Accurate modeling of joint effects in lattice transmission towers," *Engineering Structures*, vol. 33, no. 5, pp. 1817–1827, 2011.



**Hindawi**

Submit your manuscripts at  
<http://www.hindawi.com>

